Inorg. Chem. **2004**, *43*, 5761–5770

One-Dimensional Oxalato-Bridged Cu(II), Co(II), and Zn(II) Complexes with Purine and Adenine as Terminal Ligands

Juan P. García-Terán,[†] Oscar Castillo,*[,†] Antonio Luque,[†] Urko García-Couceiro,[†] Pascual Román,[†] and Francesc Lloret[‡]

Departamento de Química Inorgánica, Universidad del País Vasco, Apartado 644, E-48080 Bilbao, Spain, and Departament de Química Inorgànica/Instituto de Ciencia Molecular, Facultat de Química, Universitat de València, Dr. Moliner 50, E-46100 Burjassot, València, Spain

Received April 2, 2004

The reaction of nucleobases (adenine or purine) with a metallic salt in the presence of potassium oxalate in an aqueous solution yields one-dimensional complexes of formulas $[M(\mu\text{-ox})(H_2O)(pur)]_n$ (pur = purine, ox = oxalato ligand (2-); M = Cu(II) [**1**], Co(II) [**2**], and Zn(II) [**3**]), $[Co(\mu\text{-ox})(H_2O)(pur)_{0.76}(ade)_{0.24}]_n$ (**4**) and $\{[M(\mu\text{-ox})(H_2O)(ade)]\cdot 2(ade)\cdot(H_2O)\}_n$ (ade = adenine; M = Co(II) [**5**] and Zn(II) [**6**]). Their X-ray single-crystal structures, variable-temperature magnetic measurements, thermal behavior, and FT-IR spectroscopy are reported. The complexes **1**–**4** crystallize in the monoclinic space group $P2_1/a$ (No. 14) with similar crystallographic parameters. The compounds **5** and **6** are also isomorphous but crystallize in the triclinic space group $P\bar{1}$ (No. 2). All compounds contain one-dimensional chains in which *cis*-$[M(H_2O)(L)]^{2+}$ units are bridged by bis-bidentate oxalato ligands with M···M intrachain distances in the range 5.23–5.57 Å. In all cases, the metal atoms are six-coordinated by four oxalato oxygen atoms, one water molecule, and one nitrogen atom from a terminal nucleobase, building distorted octahedral MO_4O_wN surroundings. The purine ligand is bound to the metal atom through the most basic imidazole N9 atom in **1**–**4**, whereas in **5** and **6** the minor groove site N3 of the adenine nucleobase is the donor atom. The crystal packing of compounds **5** and **6** shows the presence of uncoordinated adenine and water crystallization molecules. The cohesiveness of the supramolecular 3D structure of the compounds is achieved by means of an extensive network of noncovalent interactions (hydrogen bonds and π–π stacking interactions). Variable-temperature magnetic susceptibility measurements of the Cu(II) and Co(II) complexes in the range 2–300 K show the occurrence of antiferromagnetic intrachain interactions.

Introduction

After the elucidation of the DNA double-helix structure by Watson and Crick[1] a great deal of attention was drawn to analyze the noncovalent forces (essentially, hydrogen bonds involving the complementary DNA bases and arene−arene π-stacking of the planar heterocycles of the nucleobases)[2] operative in the control of the conformation and the molecular recognition phenomena of a great diversity of macromolecular biological systems. Also many research efforts have been dedicated to study the interaction of nucleic acids and their constituents with metal ions which is a crucial stage in the development of new biologically active metallodrugs.[3] Many of the available information obtained to date arise from the knowledge of the structure and reactivity of biomimetic artificial systems based on transition metal complexes containing nucleobase ligands or analogues.[4] Most of these complexes are monomers or discrete polymeric species of low nuclearity in which the structural units are held together by means of the above-cited noncovalent interactions. Examples of *n*-dimensional (*n*D, $n = 1-3$) metal-organic coordination networks based solely on covalent

* Author to whom correspondence should be addressed. E-mail: qipcacao@lg.ehu.es.
[†] Universidad del País Vasco.
[‡] Universitat de València.

(1) Watson, J. D.; Crick, F. H. C. *Nature* **1953**, *171*, 737.
(2) (a) Guckian, K. M.; Schweitzer, B. A.; Ren, R. X.-F.; Sheils, C. J.; Tahmassebi, D. C.; Kool, E. T. *J. Am. Chem. Soc.* **2000**, *122*, 2213. (b) Janiak, C. *J. Chem. Soc., Dalton Trans.* **2000**, 3885. (c) Yoshizawa, S.; Kawai, G.; Watanabe, K.; Miura, K.; Hirao, I. *Biochemistry* **1997**, *36*, 4761. (d) Ren, X.-F.; Schweitzer, B. A.; Sheils, C. J.; Kool, E. T. *Angew. Chem., Int. Ed. Engl.* **1996**, *35*, 743.
(3) Berners-Price, S. J.; Sadler, P. J. *Coord. Chem. Rev.* **1996**, *151*, 1.
(4) Lippert, B. *Coord. Chem. Rev.* **2000**, *200*−*202*, 487.

10.1021/ic049569h CCC: $27.50 © 2004 American Chemical Society
Published on Web 08/30/2004

bonds are quite limited, despite the high scientific interest that such complexes, resembling DNA double helix dimensionality, might show. To the best of our knowlegde, only two 1D polymers containing nonsubstituted purine nucleobases (purine, adenine and guanine) have been structurally characterized so far: the compound $\{[Cu(\mu\text{-pur})(H_2O)_4]SO_4\cdot 2H_2O\}_n$ in which the nucleobase acts as a N7,N9 bridging ligand,[5] and the compound $[Cu_2Cl_6(H_2pur)]_n$ where the purinium dication is attached to the metal in N3-monodentate form[6] with a distance of 2.561(3) Å which is 0.53 Å longer than the average Cu−N3 bond distance found for nucleic-acid constituents containing purine bases.[4]

In previous works, and in the framework of our current research on the chemistry of polymeric complexes based on the oxalato-bridging ligand, we have set up a strategy for the design of one-dimensional complexes with the general formula $[M(\mu\text{-ox})(L)_2]_n$ containing substituted pyridine derivatives as terminal ligands.[7−10] By using similar synthetic routes now we have succeeded in preparing a novel family of 1D complexes in which the pyridinic bases are replaced by nucleobases such as purine and adenine. In the present paper, we report the syntheses and the crystal structures of these new complexes as well as their magnetic and thermal properties. In the compounds $[M(\mu\text{-ox})(H_2O)(pur)]_n$ (ox = oxalato ligand (2-); M = Cu(II) [**1**], Co(II) [**2**], and Zn(II) [**3**]) and $[Co(\mu\text{-ox})(H_2O)(pur)_{0.76}(ade)_{0.24}]_n$ (**4**) the neutral purine (pur) behaves as a N9-monodentated ligand. The only other case of transition metal ion binding to the imidazole ring N9 atom of the purine ligand has been reported in the monomer $[TiCl(cp)_2(pur)]$ (cp is the cyclopentadienyl anion) with a purinate monoanion.[11] However, there are a large number of compounds in which substituted purine ligands are coordinated to the metallic center through the imidazole N9 atom.[12,13] The adenine nucleobase (ade) in the compounds $\{[M(\mu\text{-ox})(H_2O)(ade)]\cdot 2(ade)\cdot(H_2O)\}_n$ (M = Co(II) [**5**] and Zn(II) [**6**]) is bound to the metal centers through the minor groove N3 site, and, to the best of our knowledge, they are the first examples of 1D transition metal complexes with a DNA purine nucleobase as terminal ligand. Several examples of one-dimensional polymeric complexes containing nucleosides as terminal ligands have been also reported.[14]

Experimental Section

Materials. All chemicals were of reagent grade and were used as commercially obtained. Standard literature procedures were used to prepare the starting $Co(ox)\cdot 2H_2O$ and $Zn(ox)\cdot 2H_2O$.[15] Elemental analyses (C, H, N) were performed on a LECO CHNS-932 microanalytical analyzer. Metal content was determined by absorption spectrometry.

Synthesis of $[Cu(\mu\text{-ox})(H_2O)(pur)]_n$ (1). An aqueous solution (20 mL) of $Cu(NO_3)_2\cdot 2H_2O$ (0.050 g, 0.21 mmol) was added dropwise to an aqueous solution (40 mL) of purine (0.051 g, 0.42 mmol) and $K_2(ox)\cdot H_2O$ (0.039 g, 0.21 mmol) with continuous stirring. After filtration of the slight amount of insoluble material, the resulting blue solution was allowed to evaporate at room temperature. X-ray suitable blue single-crystals of compound **1** were obtained after 4 days. Yield: 60% (based on metal). Anal. Calcd for $C_7H_6CuN_4O_5$: C, 29.02; H, 2.09; N, 19.34; Cu, 21.94. Found: C, 28.91; H, 2.12; N, 19.20; Cu, 22.04. Main IR features (cm^{-1}, KBr pellet): 3440s for ν(O−H); 3135s for $\nu(C_8-H + C_2-H)$; 1669s, 1642sh for ν_{as} (O−C−O); 1612vs for ν(C═C); 1483m for $(\delta(C_2-H + C_8-N_9) + \nu(C_8-H))$; 1403m for $\delta(N_1-C_6-H_6)$; 1354m for $\nu(C_5-N_7-C_8)$; 1288m for $(\nu(N_9-C_8 + N_3-C_2) + \delta(C-H) + \nu_s(O-C-O))$; 1263m for $(\delta(C_8-H) + \nu(N_7-C_8))$; 978m for $\nu(N_1-C_6)$; 800m for δ(O−C−O); 743m, 659w for ring deformation; 512m, 468m for ν(M−O + M−N).

Synthesis of $[Co(\mu\text{-ox})(H_2O)(pur)]_n$ (2). An aqueous solution (20 mL) of purine (0.100 g, 0.83 mmol) was added dropwise to a solution (30 mL) of $Co(ox)\cdot 2H_2O$ (0.152 g, 0.83 mmol) and $K_2(ox)\cdot H_2O$ (0.917 g, 4.98 mmol) in water with continuous stirring. The resulting red solution was allowed to evaporate at room temperature. A polycrystalline sample of compound **2** was obtained after 4 days. Yield: 70%. Red single crystals of **2** suitable for X-ray diffraction studies were grown after two weeks by the slow diffusion of an aqueous methanolic solution of purine into an aqueous solution containing $Co(ox)\cdot 2H_2O$ and $K_2(ox)\cdot H_2O$. Anal. Calcd for $C_7H_6CoN_4O_5$: C, 29.49; H, 2.12; N, 19.65; Co, 20.67. Found: C, 29.34; H, 2.12; N, 19.58; Co, 20.48. Main IR features (cm^{-1}, KBr pellet): 3355s for ν(O−H); 3140s for $\nu(C_8-H + C_2-H)$; 1664s, 1603vs for ν_{as} (O−C−O); 1614vs for ν(C═C); 1478s for $(\delta(C_2-H + C_8-N_9) + \nu(C_8-H))$; 1408s for $\delta(N_1-C_6-H_6)$; 1363m for $\nu(C_5-N_7-C_8)$; 1313s for $(\nu(N_9-C_8 + N_3-C_2) + \delta(C-H) + \nu_s(O-C-O))$; 1263s for $(\delta(C_8-H) + \nu(N_7-C_8))$; 973m for $\nu(N_1-C_6)$; 800s for δ(O−C−O); 698m, 658w for ring deformation; 503m, 468w for ν(M−O + M−N).

Synthesis of $[Zn(\mu\text{-ox})(H_2O)(pur)]_n$ (3). The preparation of **3** is analogous to that described for **2** but replacing $Co(ox)\cdot 2H_2O$ by $Zn(ox)\cdot 2H_2O$. Colorless polyhedral crystals of **3** were obtained after 4 days. Yield: 75%. Anal. Calcd for $C_7H_6ZnN_4O_5$: C, 28.84; H, 2.07; N, 19.22; Zn, 22.43. Found: C, 29.04; H, 2.10; N, 19.28; Zn, 22.39. Main IR features (cm^{-1}, KBr pellet): 3355s for ν(O−H); 3144s for $\nu(C_8-H + C_2-H)$; 1662vs, 1607vs for ν_{as} (O−C−O); 1622vs for ν(C═C); 1484s for $(\delta(C_2-H + C_8-N_9) + \nu(C_8-H))$; 1426s, 1407s for $\delta(N_1-C_6-H_6)$; 1370s for $\nu(C_5-N_7-C_8)$; 1319s, 1311s for $(\nu(N_9-C_8 + N_3-C_2) + \delta(C-H) + \nu_s(O-C-O))$; 1266s for $(\delta(C_8-H) + \nu(N_7-C_8))$; 973m for $\nu(N_1-C_6)$; 802s for δ(O−C−O); 701m, 657m for ring deformation; 512s, 500m, 467w for ν(M−O + M−N).

(5) Vestues, P. I.; Sletten, E. *Inorg. Chim. Acta* **1981**, *52*, 269.
(6) (a) Sheldrick, W. S. *Acta Crystallogr.* **1981**, *B37*, 945. (b) Sletten, E.; Sletten, J.; Froystein, N. A. *Acta Chem. Scand.* **1988**, *A42*, 413.
(7) Castillo, O.; Luque, A.; Román, P.; Lloret, F.; Julve, M. *Inorg. Chem.* **2001**, *40*, 5526.
(8) Castillo, O.; Luque, A.; Lloret, F.; Román, P. *Inorg. Chim. Acta* **2001**, *324*, 141.
(9) Castillo, O.; Luque, A.; Julve, M.; Lloret, F.; Román, P. *Inorg. Chim. Acta* **2001**, *315*, 9.
(10) Pilkington, M.; Decurtins, S. In *Comprehensive Coordination Chemistry II;* McCleverty, J. A., Meyer, T. J., Eds.; Elsevier Ltd.: University of Berne, Switzerland, 2004; Vol. 7, p 177.
(11) Beauchamp, A. L.; Cozak, D.; Mardhy, A. *Inorg. Chim. Acta* **1984**, *92*, 191.
(12) (a) Travnicek, Z.; Malon, M.; Sindelar, Z.; Dolezal, K.; Rolcik, J.; Kystof, V.; Strnad, M.; Marek, J. *J. Inorg. Biochem.* **2001**, *84*, 23. (b) Umadevi, B.; Stanley, M.; Muthiah, P. T.; Varghese, B. *Ind. J. Chem.* **2002**, *A41*, 737. (c) Valach, F.; Tokarcik, M.; Maris, T.; Watkain, D. J.; Prout, C. K. *J. Organomet. Chem.* **2001**, *622*, 166.
(13) (a) De Meester, P.; Skapski, A. C. *J. Chem. Soc., Dalton Trans.* **1973**, *15*, 1596. (b) Hanggi, G.; Schmalle, H.; Dubler, E. *Acta Crystallogr.* **1992**, *C48*, 1008.
(14) (a) Authier-Martin, M.; Hubert, J.; Rivest, R.; Beauchamp, A. L. *Acta Crystallogr.* **1978**, *B34*, 273. (b) Quirós-Olozabal, M.; Salas-Peregrín, J. M.; Sánchez, M. P.; Faure, R. *An. Quim.* **1990**, *86*, 518.
(15) (a) Remy, H. In *Treatise on Inorganic Chemistry*; VCH: Weinheim, Germany, 1956. (b) Kirschner, S. In *Inorganic Synthesis*; Rochow, E. G., Ed.; McGraw-Hill Book Co.: New York, 1960; Vol. VI.

Synthesis of $[Co(\mu-ox)(H_2O)(pur)_{0.76}(ade)_{0.24}]_n$ (4). Red single crystals of **4** were prepared by the slow diffusion of an aqueous methanolic solution of purine (0.079 g, 0.66 mmol) and adenine (0.089 g, 0.66 mmol) into an aqueous solution of Co(ox)·$2H_2O$ (0.120 g, 0.66 mmol) and K_2(ox)·H_2O (0.729 g, 3.96 mmol). Crystal growth was observed after three weeks. Yield: 30%. Anal. Calcd for $C_7H_{6.24}CoN_{4.24}O_5$: C, 29.12; H, 2.18; N, 20.57; Co, 20.41. Found: C, 28.98; H, 2.16; N, 20.58; Co, 20.47. Main IR features (cm^{-1}, KBr pellet): 3420s for ν(O−H); 3380s for ($\nu(NH_2)$ + $(2\delta NH_2)$); 3140s for ($\nu(C_8-H + C_2-H) + \nu NH_2$); 1660s, 1649sh for ν_{as} (O−C−O); 1614vs, 1603sh for (ν(C═C) + (δNH_2)); 1479s for ($\delta(C_2-H + C_8-N_9) + \nu(C_8-H)$); 1405s for $\delta(N_1-C_6-H_6)$; 1361m for $\nu(C_5-N_7-C_8)$; 1313s for ($\nu(N_9-C_8 + N_3-C_2)$ + δ(C−H) + ν_s(O−C−O)); 1263m for ($\delta(C_8-H) + \nu(N_7-C_8)$); 1028m for $\tau(NH_2)$; 968m for ($\nu(N_1-C_6) + \tau(NH_2)$); 800s for δ(O−C−O); 704w, 665m for ring deformation; 503m, 463w for ν(M−O + M−N).

Synthesis of $\{[Co(\mu-ox)(H_2O)(ade)]\cdot 2(ade)\cdot(H_2O)\}_n$ (5). An aqueous methanolic solution (45 mL) of adenine (0.120 g, 0.88 mmol) was added dropwise to an aqueous solution containing 30 mL of Co(ox)·$2H_2O$ (0.054 g, 0.30 mmol) and K_2(ox)·H_2O (0.327 g, 1.78 mmol) with continuous stirring at 50 °C. The resulting red solution was allowed to evaporate at room temperature. Single crystals of compound **5** were obtained after 4 days. Yield: 40%. Anal. Calcd for $C_{17}H_{19}CoN_{15}O_6$: C, 34.70; H, 3.23; N, 35.71; Co, 10.02. Found: C, 34.54; H, 3.19; N, 35.63; Co, 9.89. Main IR features (cm^{-1}, KBr pellet): 3445s for ν(O−H); 3348s, 3258s for ($\nu(NH_2)$ + $(2\delta NH_2)$); 3111s for ($\nu(C_8-H + C_2-H) + \nu NH_2$); 1689s, 1660sh for ν_{as} (O−C−O); 1609vs for (ν(C═C) + (δNH_2)); 1584sh for ($\nu(C_4-C_5) + N_3-C_4-C_5$)); 1478m for ($\delta(C_2-H + C_8-N_9) + \nu(C_8-H)$); 1418m for $\delta(N_1-C_6-H_6)$; 1343m for $\nu(C_5-N_7-C_8)$; 1308s for ($\nu(N_9-C_8 + N_3-C_2) + \delta$(C−H) + ν_s(O−C−O)); 1243m for ($\delta(C_8-H) + \nu(N_7-C_8)$); 1028w for $\tau(NH_2)$; 973w for ($\nu(N_1-C_6) + \tau(NH_2)$); 800m for δ(O−C−O); 693m, 653w for ring deformation; 508w, 463w for ν(M−O + M−N).

Synthesis of $\{[Zn(\mu-ox)(H_2O)(ade)]\cdot 2(ade)\cdot(H_2O)\}_n$ (6). This compound was prepared by following an analogous procedure to that for **5**, but using Zn(ox)·$2H_2O$ as starting material. Single crystals of compound **6** were obtained after 4 days. Yield: 50%. Anal. Calcd for $C_{17}H_{19}ZnN_{15}O_6$: C, 34.33; H, 3.22; N, 35.32; Zn, 10.99. Found: C, 34.27; H, 3.20; N, 35.36; Zn, 10.97. Main IR features (cm^{-1}, KBr pellet): 3444s for ν(O−H); 3349s, 3263s for ($\nu(NH_2)$ + $(2\delta NH_2)$); 3107s for ($\nu(C_8-H + C_2-H) + \nu NH_2$); 1692s, 1657sh for ν_{as} (O−C−O); 1606vs for (ν(C═C) + (δNH_2)); 1586s for ($\nu(C_4-C_5) + N_3-C_4-C_5$)); 1478m for ($\delta(C_2-H + C_8-N_9) + \nu(C_8-H)$); 1416m for $\delta(N_1-C_6-H_6)$; 1345s for $\nu(C_5-N_7-C_8)$; 1322s, 1305s for ($\nu(N_9-C_8 + N_3-C_2) + \delta$(C−H) + ν_s(O−C−O)); 1249m, 1240m for ($\delta(C_8-H) + \nu(N_7-C_8)$); 1028m for $\tau(NH_2)$; 956w for ($\nu(N_1-C_6) + \tau(NH_2)$); 798m for δ(O−C−O); 694m, 675m, 656m, 641m, 625m for ring deformation; 513m, 465w for ν(M−O + M−N).

Physical Measurements. The IR spectra (KBr pellets) were recorded on a FTIR Mattson 1000 spectrometer in the 4000−400 cm^{-1} spectral region. Thermal analyses (TG/DTG/DTA) were performed on a TA Instruments STD 2960 thermal analyzer in a synthetic air atmosphere (79%N_2/21%O_2) with a heating rate of 5 °C min^{-1}. Magnetic measurements were performed on polycrystalline samples of the compounds with a Quantum Design SQUID susceptometer covering the temperature range of 2.0−300 K. The susceptibility data were corrected for the diamagnetism estimated from Pascal's tables,[16] the temperature-independent paramagnetism, and the magnetization of the sample holder.

X-ray Data Collection and Structure Determination. Data collections on single crystals of all compounds were carried out at 293(2) K with an Xcalibur diffractometer, with the exception of compound **1**, which was measured on a Bruker-Nonius KappaCCD2000 diffractometer. Both diffractometers were equipped with an area detector, using graphite monochromated MoKα radiation (λ = 0.71073 Å) on the Xcalibur diffractometer and graphite monochromated CuKα radiation (λ = 1.54178 Å) on the Bruker-Nonius KappaCCD2000 diffractometer. Data were corrected for Lorentz and polarization effects. No absorption correction was applied. Neutral atom scattering factors and anomalous dispersion factors were taken from the literature.[17] The structures were solved by direct methods using the SIR 97 program.[18] Full matrix least-squares refinements were performed on F^2 using SHELXL97.[19] The refinement of structural model of **4** indicates the existence of a randomly partial substitution of the purine by adenine. A substantial maximum in the difference Fourier map was found at a distance of ca. 1.2 Å from atom C6, along with the expected peak at the typical C−H distance. The constrained refinement of the H6 (purine) and N6 (adenine) atoms indicated that 24% of H6-atom sites in the crystal were occupied by an amino group. The sum of the occupancy parameters of the H6 atom and the atoms of the amino group was constrained to be 1.0. The coordinates of the two hydrogen atoms of the disordered amino group were calculated and were included in the final cycles of the refinement using a riding model. All non-hydrogen atoms were refined anisotropically. All calculations were performed using the WinGX crystallographic software package.[20] The final geometrical calculations and the graphical manipulations were carried out with the PARST95[21] and PLATON[22] programs. Crystallographic data for compounds are given in Tables 1 and 2.

Results and Discussion

Description of the Structures. The main structural feature common to all compounds is the presence of one-dimensional *zigzag* chains (Figure 1) in which *cis*-$[M(H_2O)(L)]^{2+}$ units are sequentially bridged by two bis-bidentate centrosymmetric oxalato ligands (*ox1* and *ox2*) with dihedral angles between two consecutive ones of about 90° (**1**−**4**) and 80° (**5** and **6**). The M···M intrachain distances across the oxalato bridges vary from 5.236(2) Å [**1**] to 5.574(1) Å [**6**]. A perspective view of the polymeric chains is given in Figure 1, whereas selected bond lengths are gathered in Table 3. The numbering system here used for the nucleobases is that conventionally accepted for chemical and biological purposes. The metal atoms (placed on a general position) exhibit a distorted octahedral coordination formed by four oxygen atoms from two bridging oxalato ligands, one water molecule, and one endocyclic nitrogen atom of the nucleobase in the cis position, resulting in a MO_4O_wN donor set.

(16) Earnshaw, A. *Introduction to Magnetochemistry*; Academic Press: London, 1968.
(17) *International Tables for X-ray Crystallography*; Kynoch: Birmingham, England, 1974; Vol. IV, p 99.
(18) Altomare, A.; Burla, M. C.; Camalli, M.; Cascarano, G. L.; Giacovazzo, C.; Guagliardi, A.; Moliterni, A. G. G.; Spagna, R. *J. Appl. Crystallogr.* **1999**, *32*, 115.
(19) Sheldrick, G. M. *SHELXS97 and SHELXL97*; University of Göttingen, Germany, 1997.
(20) Farrugia, L. J. *WINGX. A Windows program for crystal structure analysis*; University of Glasgow: Great Britain, 1998.
(21) Nardelli, M. *J. Appl. Crystallogr.* **1995**, *28*, 659.
(22) Spek, A. L. *PLATON, a multipurpose crystallographic tool*; Utrecht University: Utrecht, Holland, 1998.

Table 1. Single-Crystal Data and Structure Refinement Details for Compounds **1**−**4**[a]

	1	**2**	**3**	**4**
formula	$C_7H_6CuN_4O_5$	$C_7H_6CoN_4O_5$	$C_7H_6ZnN_4O_5$	$C_7H_{6.24}CoN_{4.24}O_5$
w (g mol^{-1})	289.70	285.09	291.53	288.68
λ (Å)	1.54178	0.71073	0.71073	0.71073
space group	$P2_1/a$	$P2_1/a$	$P2_1/a$	$P2_1/a$
a (Å)	7.277(2)	6.9489(4)	6.988(1)	6.897(1)
b (Å)	15.929(3)	16.1481(11)	16.143(2)	16.457(2)
c (Å)	8.263(2)	8.3511(5)	8.334(1)	8.308(1)
β (°)	106.06(3)	105.956(6)	106.10(1)	106.14(1)
V (Å^3)	920.4(4)	901.0(1)	903.3(2)	905.8(2)
Z	4	4	4	4
μ (mm^{-1})	3.614	1.925	2.739	1.925
D_{obsd} (Mg m^{-3})	2.08(1)	2.09(1)	2.13(1)	2.12(1)
D_{calcd} (Mg m^{-3})	2.091	2.102	2.144	2.115
refl. collected	5486	7125	7681	7173
indep. refl.	1359	2614	2640	2639
$\Delta\rho$max,min (e Å^{-3})	0.34, −0.63	0.45, −0.39	0.80, −0.34	0.56, −0.61
final R[b] indexes	R1 = 0.0411	R1 = 0.0353	R1 = 0.0373	R1 = 0.0433
[I > 2 σ(I)]	wR2 = 0.1178	wR2 = 0.0871	wR2 = 0.0764	wR2 = 0.0730
R indexes	R1 = 0.0412	R1 = 0.0360	R1 = 0.0677	R1 = 0.0813
(all data)	wR2 = 0.1179	wR2 = 0.0876	wR2 = 0.0836	wR2 = 0.0886

[a] Details in common: T = 293(2) K, D_{obsd} measured in $CCl_4/CHBr_3$. [b] $R1 = \Sigma||F_o| - |F_c||/\Sigma|F_o|$. $wR2 = [\Sigma w(F_o^2 - F_c^2)^2/\Sigma w(F_o^2)^2]^{1/2}$.

Table 2. Single-Crystal Data and Structure Refinement Details for Compounds **5** and **6**[a]

	5	**6**
formula	$C_7H_7CoN_5O_5\cdot 2(C_5H_5N_5)\cdot(H_2O)$	$C_7H_7ZnN_5O_5\cdot 2(C_5H_5N_5)\cdot(H_2O)$
w (g mol^{-1})	588.4	594.84
λ (Å)	0.71073	0.71073
space group	$P\bar{1}$	$P\bar{1}$
a (Å)	7.471(1)	7.487(2)
b (Å)	8.210(1)	8.226(2)
c (Å)	19.099(2)	19.150(2)
α(°)	82.34(1)	82.06(2)
β (°)	80.23(1)	80.16(2)
γ (°)	74.62(1)	74.40(2)
V (Å^3)	1108.3(2)	1114.0(4)
Z	2	2
μ (mm^{-1})	0.849	1.177
D_{obsd} (Mg m^{-3})	1.76(1)	1.78(1)
D_{calcd} (Mg m^{-3})	1.763	1.773
refl. collected	10650	11012
indep. refl.	6335	6430
$\Delta\rho$max,min (e Å^{-3})	0.42, −0.49	0.44, −0.44
final R[b] indexes	R1 = 0.0476	R1 = 0.0425
[I > 2 σ(I)]	wR2 = 0.0735	wR2 = 0.0730
R indexes	R1 = 0.0772	R1 = 0.0580
(all data)	wR2 = 0.0872	wR2 = 0.0711

[a] Details in common: T = 293(2) K, D_{obsd} measured in $CCl_4/CHBr_3$. [b] $R1 = \Sigma||F_o| - |F_c||/\Sigma|F_o|$. $wR2 = [\Sigma w(F_o^2 - F_c^2)^2/\Sigma w(F_o^2)^2]^{1/2}$.

$[M(\mu\text{-ox})(H_2O)(pur)]_n$ (M = Cu (1), Co (2), Zn (3)) and $[Co(\mu\text{−ox})(H_2O)(pur)_{0.76}(ade)_{0.24}]_n$ (4). Compounds **1**−**4** are isomorphous and crystallize in the monoclinic space group $P2_1/a$. Their crystallographic parameters are similar except for compound **4,** which shows a slight elongation of the *b* crystallographic parameter [16.148(1) Å for **2** vs 16.457(2) Å for (**4**)] due to the randomly partial substitution of purine ligands for adenine ligands, with 76% and 24% occupation rates, respectively. The most striking difference between the polymeric chains is the expected tetragonal Jahn−Teller elongation of the copper(II) octahedron in **1**, with two trans axial bonds distances [Cu−O5w: 2.402(3) Å and Cu−O1: 2.277(2) Å] substantially longer than the equatorial ones (ca. 2.00 Å). Compounds **2**−**4** exhibit a rather typical octahedral metal(II) coordination with quite regular metal−ligand bond distances. The M−O_{ox} bond distances are in the expected range [Co: 2.079(2)-2.124(2) Å, Zn: 2.075(2)-2.142(2) Å] in comparison with other polynuclear oxalato-bridged cobalt(II) and zinc(II) complexes.[23−25] The nucleobase ligand is coordinated to the metal through the N9 atom of the imidazole ring. The Cu−N9 bond distance in the copper(II) complex [2.009(3) Å] is somewhat shorter than those found for compounds **2**−**4** (ca. 2.12 Å), but it is similar to that

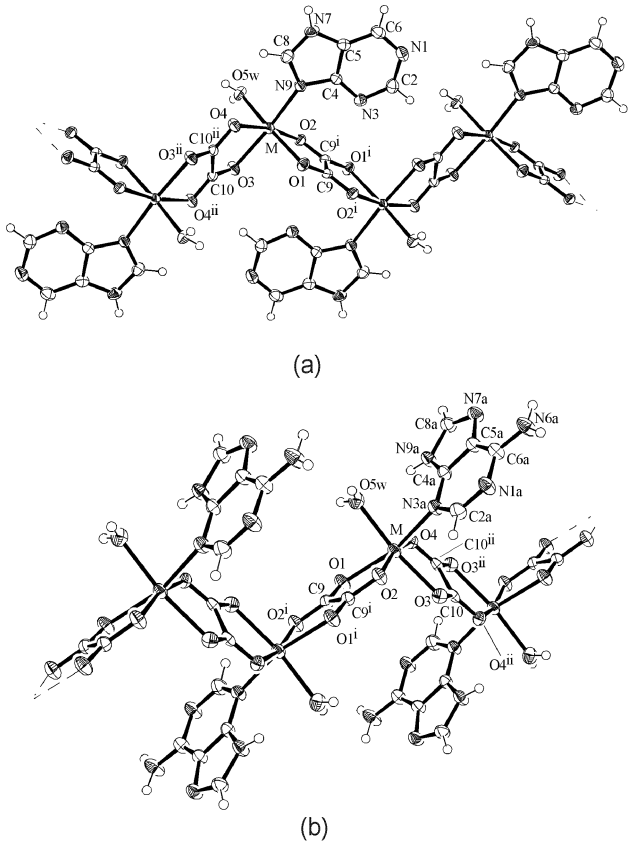

Figure 1. Perspective drawing of the polymeric chain of (a) **1** and (b) **5**. Displacement ellipsoids are drawn at the 50% probability level. Symmetry codes for **1** (i) -x + 1, -y, -z + 1; (ii) -x + 2, -y, -z + 2. Symmetry codes for **5** (i) -x + 1, -y, -z; (ii) -x, -y + 1, -z.

Table 3. Selected Bond Lengths (Å) and Angles (deg)

	1	2	3	4	5	6
M−O1	2.277(2)	2.098(1)	2.107(2)	2.093(2)	2.123(2)	2.143(2)
M−O2	1.967(2)	2.081(1)	2.075(2)	2.079(2)	2.067(2)	2.052(2)
M−O3	2.019(2)	2.121(1)	2.142(2)	2.124(2)	2.158(2)	2.177(3)
M−O4	1.994(2)	2.102(2)	2.091(2)	2.095(2)	2.108(2)	2.097(2)
M−O5w	2.402(3)	2.109(2)	2.120(2)	2.109(2)	2.087(2)	2.116(2)
M−NX[a]	2.009(3)	2.124(2)	2.117(2)	2.121(3)	2.112(2)	2.114(3)
O1−M−O2	79.1(1)	80.40(5)	80.47(8)	80.7(1)	79.9(1)	79.89(9)
O1−M−O3	90.5(1)	90.89(6)	91.39(9)	91.4(1)	100.8(1)	100.72(9)
O1−M−O4	102.0(1)	94.36(6)	94.06(9)	92.8(1)	93.2(1)	92.34(9)
O1−M−O5w	163.8(1)	171.76(6)	170.41(8)	171.5(1)	84.7(1)	83.98(9)
O1−M−NX	93.1(1)	90.40(6)	91.29(9)	90.8(1)	164.4(1)	163.67(10)
O2−M−O3	90.8(1)	92.10(6)	91.46(8)	92.0(1)	89.7(1)	89.42(9)
O2−M−O4	173.6(1)	169.65(6)	168.52(7)	168.8(1)	164.4(1)	163.41(9)
O2−M−O5w	84.8(1)	91.38(6)	89.94(9)	90.8(1)	100.5(1)	101.86(9)
O2−M−NX	96.7(1)	96.15(6)	97.39(8)	95.7(1)	95.3(1)	95.95(10)
O3−M−O4	82.9(1)	78.99(5)	78.51(8)	79.0(1)	77.8(1)	77.55(8)
O3−M−O5w	89.4(1)	89.93(6)	89.05(8)	89.3(1)	169.2(1)	168.43(8)
O3−M−NX	172.2(1)	171.75(6)	171.06(8)	172.2(1)	94.0(1)	94.99(10)
O4−M−O5w	94.0(1)	93.84(6)	95.41(9)	95.7(1)	92.7(1)	91.77(9)
O4−M−NX	89.6(1)	92.79(6)	92.80(8)	93.5(1)	94.9(1)	95.39(10)
O5w−M−NX	89.1(1)	89.97(6)	89.72(9)	89.7(1)	81.6(1)	81.43(10)

[a] NX = N9 (**1**−**4**), N3a (**5** and **6**).

[2.023(1) Å] seen in the compound $[CuCl_3(HL)_2]Cl\cdot 2H_2O$ where the protonated 6-(3-chlorobenzylamino)purine ligand shows the same binding site.[12a] Although numerous examples exist of well structurally characterized metal complexes of substituted purine derivatives, only five structures in which purine itself is coordinated to metal ions have been retrieved from the Cambridge structural database (CSD, January 2004 release)[26] probably due to that this ligand is not a natural DNA nucleobase. As commented on in the Introduction, two one-dimensional Cu(II) complexes exhibit purine ligands coordinated to the metallic center in N3-monodentate and N7,N9-bridging forms, respectively.[5,6] In the referred [TiCl-$(cp)_2$(pur)] compound, the N9 site of the purinate monoanion is coordinated in monodentate fashion to the Ti(IV) atom with a distance of 2.132(2) Å.[11] In the two remaining structures, trichloropuriniumzinc(II)[27] and dichloropurinezinc(II),[28] the base is coordinated to the metal ions through the imidazole N7 donor atom with a bond distance of about 2.02 Å. As far as we are aware, no examples of crystallographically characterized Co(II)−purine complexes have been reported so far. However, the Co−N9 bond distances in compounds **2** and **4** are comparable to those reported for the compounds $(Hade)_2[Co(H_2O)_4(ade)_2](SO_4)\cdot 2H_2O$ (Co−N9: 2.163 Å)[13a] and $\{[Co_2(\mu\text{-hypoxantine})(SO_4)(\mu\text{-}H_2O)_2(H_2O)_2]$ (Co−N9: 2.124 Å, Co−N3: 2.163 Å).[13b]

The crystal packing of compounds **1**−**4** (Figure 2) is quite similar with a supramolecular 3D structure sustained by an extensive network of noncovalent interactions between neighboring chains (see Supporting Information). The polymeric chains run along the *[101]* direction, and they are

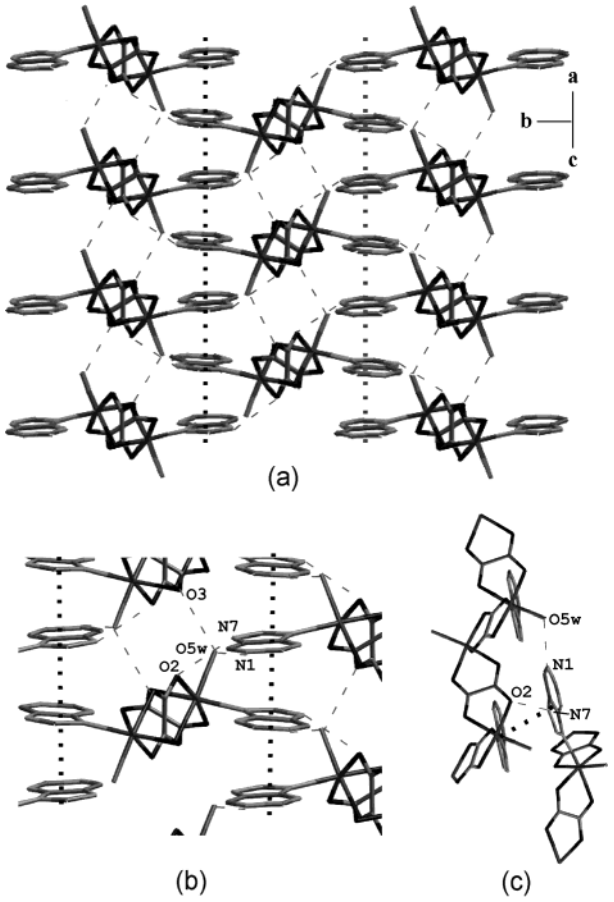

Figure 2. Hydrogen bonds (dashed lines) and $\pi-\pi$ stacking (dotted line) interactions in the crystal packing of compounds **1**−**4**.

interconnected through short hydrogen bonds of type Ow-H···O(ox) involving the coordinated O5w water molecules and the oxalato O3 atom (*ox2*) giving rise to sheets which are spreading out along the crystallographic *ac*-plane. The purine ligands are projected forward to the outside of the layers along the *b*-direction and cross-link adjacent sheets by means of two hydrogen bonds: O5w−H1w···N1 (as

(23) Glerup, J.; Goodson, P. A.; Hodgson, D. J.; Michelsen, K. *Inorg. Chem.* **1995**, *34*, 6255.
(24) Lu, J. Y.; Lawandy, M. A.; Li, J.; Yuen, T.; Lin, C. *Inorg. Chem.* **1999**, *38*, 2695.
(25) Yuen, T.; Lin, C. L.; Mihalisin, T. W.; Lawandy, M. A.; Li, J. *J. Appl. Phys.* **2000**, *87*, 6001.
(26) Allen, F. H. *Acta Crystallogr.* **2002**, *B58*, 380.
(27) Sheldrick, W. S. Z. *Naturforsch., Teil B* **1982**, *37*, 653.
(28) Laity, H. L.; Taylor, M. R. *Acta Crystallogr.* **1995**, *C51*, 1791.

acceptor) and N7−H7···O2 (as donor). The orientation of the terminal purine ligands and the partial replacement of purine by adenine (6-aminopurine) with an additional exocyclic amino group results in a slight increasing of the distance between the sheets for the compound **4** and, as a consequence, the unit cell *b* parameter is longer by ca. 0.3 Å than that found for compound **2.** The overall 3D supramolecular structure is again stabilized by significant offset face-to-face $\pi-\pi$ stacking interactions between the aromatic rings of purine bases belonging to adjacent layers with interplanar distances of around 3.3 Å. There is no evidence of hydrogen-bond interactions between purine ligands belonging to adjacent chains. It should be pointed out that the parallel orientation of the purine ligands with respect to the metal-oxalato framework locates the nonprotonated minor groove N3 atom on the carbon−carbon bond of the centrosymmetric *ox1* ligand with a mean N3···C distance of 3.0 Å and a dihedral angle between the pyrimidinic ring and the oxalato plane of about 90°. This fact precludes the involvement of the potential hydrogen-bonding N3 atom in any other interaction. A similar perpendicular arrangement of oxalato dianions and N-containing aromatic rings has been previously observed in some mixed oxalate/phenanthroline metal complexes.[29]

$\{[M(\mu-ox)(H_2O)(ade)]\cdot 2(ade)\cdot(H_2O)\}_n$ (M = Co (5), Zn (6)). Compounds **5** and **6** crystallize in the triclinic space group $P\bar{1}$ with similar unit cell parameters. The *zigzag* polymeric chains of compounds **5** and **6** grow along the crystallographic *a*-axis, and they are also comprised of *cis*-$[M(H_2O)(ade)]^{2+}$ units bridged by bis-bidentate oxalato ligands (Figure 1) with M−O bond distances similar to those previously described for compounds **2**−**4**. However, the individual polymeric chains exhibit a markedly different topology relative to the purine complexes. The most striking differences are seen with regard to the nucleobase donor sites and their orientation in the polymer chain. The natural adenine nucleobase binds to the metal centers through the less basic pyrimidinic N3 atom in contrast to what occurs in compounds **1**−**4** where the purine ligands are coordinated through the imidazole N9 atom. Among the DNA nucleobases, adenine exhibits the most versatile coordination properties.[4] The binding of metal ions to the most basic N9 donor atom of the adenine nucleobase ($pK_a = 9.8$)[30] is largely supported from a structural point of view[31−33] as could be found in a CSD search for nearly 30 compounds, and the shift of the hydrogen atom to the pyrimidinic N1 atom or the major groove N7 position is observed for neutral ligands. This fact is in agreement with the relative basicity of the N-rich adenine nucleobase (N9 > N1> N7 > N3 > N6-exocyclic).[4] So far, there are only two structurally characterized examples of Co(II)−adenine complexes and both show a N9-coordination mode of the DNA nucleobase.[27,32] The monodentate coordination mode through the minor groove N3 site is likewise less common, and it has been described[34−36] for several compounds containing Cu, Pd, and Ni. It usually stems from steric effects around the metal atom and/or the presence of noncovalent interactions stabilizing the crystal structure. One such example is the complex [Cu(MOBIDA)(ade)$(H_2O)]\cdot H_2O$[35] (MOBIDA is the *N*-(*p*-methoxybenzyl)-iminodiacetato(2-) ligand) in which the unusual N3-coordination of the nucleobase is controlled by a molecular recognition process involving the formation of an intramolecular interligand N7(imidazole-like)-H···O(carboxyl) hydrogen-bond and the intermolecular interligand $\pi-\pi$ stacking interaction between the six membered rings of benzyl (MOBIDA) and the adenine ligands. As far as we are aware, this type of binding has not been previously observed for Zn(II)−adenine complexes.[33,37] Hydrated alkali metal ion binding to the N3 position of adenine (in conjunction with O2 of thymine) in the minor groove of DNA has lately received attention in some hydration processes of the B-DNA.[4] For adenine derivatives, however, there is an increasing number of reports of metal ions binding at this less basic site.[38]

On the other hand, while in compounds **1**−**4** the bases are arranged along the growing axis of the polymeric chain, the coordinated adenine molecules in compounds **5** and **6** are almost perpendicular to the metal-oxalato framework with a dihedral angle between the adenine mean plane and the adjacent oxalato ligands of 155° (*ox1*) and 88° (*ox2*), respectively. Figure 3 shows a ball representation of the polymeric chains to highlight the polymer shape. This feature results in the presence of bulkier chains in **5** and **6** which

(29) Russell, V.; Craig, D.; Scudder, M.; Dance, I. *Cryst. Eng. Comm*. **2001**, *24*, 1.

(30) Taqui-Khan, M. M.; Krishnamoorhy, C. K. *J. Inorg. Nucl. Chem.* **1971**, *42*, 1417.

(31) (a) De Meester, P.; Skapski, A. C. *J. Chem. Soc., Dalton Trans.* **1973**, *4*, 424. (b) Brown, D. B.; Hall, J. W.; Helis, H. M.; Walton, E. G.; Hodgson, D. J.; Hatfield, W. E. *Inorg. Chem.* **1977**, *16*, 2675. (c) Sakaguchi, H.; Anzai, H.; Furuhata, K.; Ogura, H.; Titaka, Y.; Fujita, T.; Sakaguchi, T. *Chem. Pharm. Bull.* **1978**, *26*, 2465. (d) Beck, W. M.; Calabrese, J. C.; Kottmair, N. D. *Inorg. Chem.* **1979**, *18*, 176. (e) Prizant, L.; Olivier, M. J.; Rivest, R.; Beauchamp, A. L. *Can. J. Chem.* **1981**, *59*, 1311. (f) Charland, J.-P.; Beauchamp, A. L. *Croat. Chem. Acta* **1984**, *57*, 679. (g) Rosopulos, Y.; Nagel, U.; Beck, W. *Chem. Ber.* **1985**, *118*, 931. (h) Tiekink, E. R. T.; Kurucsev, T.; Hoskins, B. F. *J. Crystallogr. Spectrosc. Res.* **1989**, *19*, 823. (i) Marzotto, A.; Ciccarese, A.; Clemente, D. A.; Valle, G. *J. Chem. Soc., Dalton Trans.* **1995**, 1461. (j) Salam, M. A.; Aoki, K. *Inorg. Chim. Acta* **2001**, *314*, 71. (k) Morel, A. C.; Choquesillo-Lazarte, D.; Alarcón-Payer, C.; González-Pérez, J. M.; Castiñeiras, A.; Niclós-Gutiérrez, J. *Inorg. Chem. Commun.* **2003**, *6*, 1354.

(32) Kistenmacher, T. J. *Acta Crystallogr.* **1974**, *B30*, 1610.

(33) Badura, D.; Vahrenkamp, H. *Inorg. Chem.* **2002**, *41*, 6013.

(34) Marzotto, A.; Clemente, D. A.; Ciccarese, A.; Valle, G. *J. Crystallogr. Spectrosc.* **1993**, *23*, 119; Kickam, J. E.; Loeb, S. J.; Murphy, S. L. *Chem. Eur. J.* **1997**, *3*, 1203.

(35) Sánchez-Moreno, M. J.; Choquesillo-Lazarte, D.; González-Pérez, J. M.; Carballo, R.; Castiñeiras, A.; Niclós-Gutiérrez, J. *Inorg. Chem. Commun.* **2002**, *5*, 800.

(36) (a) Rojas-González, P. X.; Castiñeiras, A.; González-Pérez, J. M.; Choquesillo-Lazarte, D.; Niclós-Gutiérrez, J. *Inorg. Chem.* **2002**, *41*, 6190. (b) Bugella-Altamirano, E.; Choquesillo-Lazarte, D.; González-Pérez, J. M.; Sánchez-Moreno, M. J.; Marín-Sánchez, R.; Martín-Ramos, J. D.; Covelo, B.; Carballo, R.; Castiñeiras, A.; Niclós-Gutiérrez, J. *Inorg. Chim. Acta* **2002**, *339*, 160

(37) (a) Taylor, M. R. *Acta Crystallogr.* **1973**, *B29*, 884. (b) Taylor, M. R.; Westphalen, J. A. *Acta Crystallogr.* **1981**, *A37*, 63. (c) Muthiah, P. T.; Mazumdar, S. K.; Chaudhuri, S. *J. Inorg. Biochem.* **1983**, *19*, 237. (d) Taylor, M. R.; Vilkins, L. M.; McCall, M. J. *Acta Crystallogr.* **1989**, *C45*, 1625.

(38) (a) Meiser, C.; Song, B.; Freisinger, E.; Peilert, M.; Sigel, H.; Lippert, B. *Chem. Eur. J.* **1997**, *3*, 388. (b) Kickham, J. E.; Loeb, S. J.; Murphy, S. L. *Chem. Eur. J.* **1997**, *3*, 1203. (c) Shipman, M. A.; Price, C.; Elsegood, M. R.; Clegg, W.; Houlton, A. *Angew. Chem., Int. Ed.* **2000**, *39*, 2360.

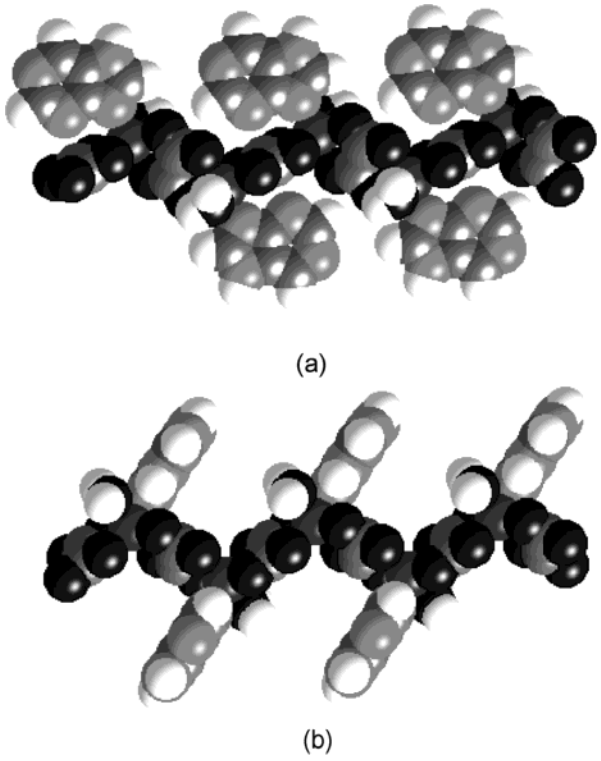

Figure 3. Balls representation of the polymeric chain topologies in **2** and **5** (above and below, respectively).

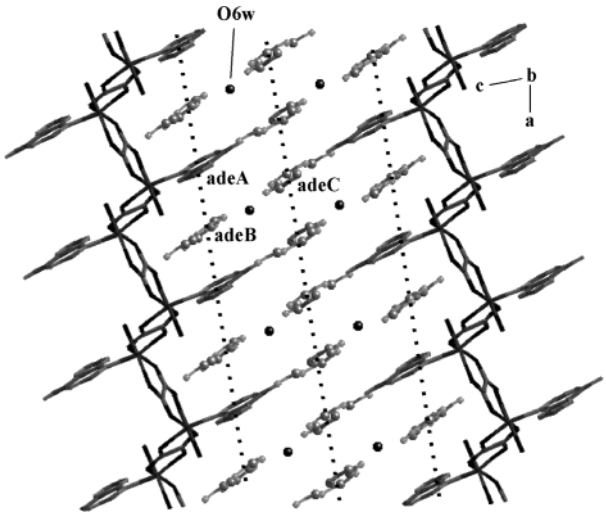

Figure 4. Crystal packing in the *ac*-plane of the compounds **5** and **6**.

leads to a less effective packing with crystallization water molecules and noncoordinated adenine molecules inserted between the chains (Figure 4). Indeed, the density values of compound **5** and **6** are smaller than those found for the purine complexes (**1**−**4**).

In the crystal packing of **5** and **6**, uncoordinated adenine molecules and the crystallization water form an intricate network of hydrogen-bonds and $\pi-\pi$ stacking interactions between them and with the chains located around them. The structural parameters of these noncovalent interactions are tabulated in the Supporting Information. The one-dimensional *zigzag* chains are linked together by means of one hydrogen-bond involving the coordinated water molecule and one oxalate oxygen atom from an adjacent chain, giving rise to

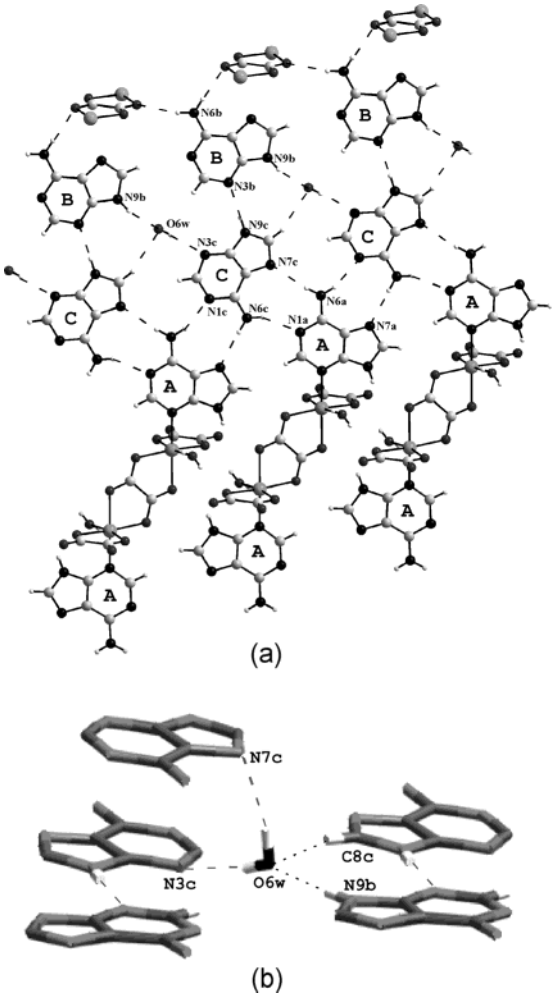

Figure 5. (a) Hydrogen-bonds involving coplanar adenine molecules in compounds **5** and **6**. (b) Hydrogen-bonding enviroment around crystallization water molecules.

sheets parallel to crystallographic plane *ab*. The interplanar distance of 7.52 Å between two consecutive parallel adenine ligands (*adeA*) in the same side of the polymeric chain permits the insertion of free adenine molecules (*adeB*) between and approximately parallel to them with a mean *adeA*-*adeB* separation of 3.22 Å (Figure 4). This value is somewhat shorter than that found between two consecutive nucleobases in the B-DNA double helix (3.4 Å). The *adeB* molecules reinforce the structural cohesiveness of the sheets by means of two hydrogen bonds between the exocyclic amino group and the oxalato O3 oxygen atoms belonging to two adjacent chains placed in the same plane.

In addition, columns of parallel stacked adenine molecules (*adeC*) are placed between the sheets of polymeric chains and *adeB* molecules, establishing themselves face-to-face $\pi-\pi$ stacking interactions with interplanar distances of about 3.5 Å. Each *adeC* molecule is surrounded by one uncoordinated *adeB* molecule and two coordinated *adeA* ligands. It establishes with them five coplanar hydrogen bonds (Figure 5). The N9c−H group forms a strong hydrogen bond to the pyrimidinic N3b atom from a *adeB* molecule, whereas the interaction with the two *adeA* ligands implies to the donor and acceptor sites of both Watson−Crick (N1 and N6 atoms)

and Hoogsteen (N7 and N6 atoms) edges of the *adeA* and *adeC* molecules to give a *zigzag* molecular array. Adenine moieties interacting via Watson−Crick···Hoogsteen face hydrogen bonding (N1/HN6···HN6/N7) to form a *zigzag* arrangement have been also found in the compound [Cu(adeninato)(tren)](ClO$_4$) (tren = tris(2-aminoethyl)amine)[39] and Rh(III) and Pt(II) complexes based on N3-bound adenine derivatives.[40] The crystal packing of the polymeric chains and free adenine molecules generates holes which are occupied by crystallization water molecules. The O6w water molecule is surrounded by three coplanar uncoordinated adenine molecules, and it is hydrogen-bonded to them. It acts as a hydrogen-bond acceptor for a N9b−H group and behaves as a donor one for the pyrimidinic N3c atom from a free *adeC* molecule. Furthermore, it is connected to an adjacent *adeC* molecule with a weak C8c−H···O6w interaction. The quite common distorted tetrahedral geometry around crystallization water molecules is achieved by a strong hydrogen bond formed between the remaining water hydrogen atom and the major groove N7c atom of one *adeC* molecule placed on a parallel plane. The hydration of DNA bases has been the subject of a large number of theoretical and experimental studies using different methods[41] to gain an insight into the special role that the interaction of nucleobases with water molecules plays in the conformation and activity of biological macromolecules.

Finally, it is interesting to note that the intercalation of the *adeB* molecules between two *adeA* ligands places the major groove N7b atom pointing at the carbon−carbon bond of one oxalato bridge with distances to both carbon atoms of 3.039 and 3.068 Å. Indeed, the imidazole N7b atom is not part of the above-described network of hydrogen-bonds, similarly to the N3 site in **1**−**4** compounds.

Thermal Stability. The thermal behavior of the compounds has been deduced from their TG and DTA curves in synthetic air (see Supporting Information). The thermal analysis of compound **1** shows a first weight loss in an endothermic process between 110 and 135 °C, attributable to the loss of the coordinated water molecule (exp. 5.9%, calc. 6.2%). The resulting compound is stable up to 150 °C, and then it undergoes successive decomposition processes to yield CuO above 400 °C. The lower stability of compound **1** may be attributable to the weakness of the Cu−Ow bond owing to the Jahn−Teller effect present in the Cu(II) coordination polyhedron. On the other hand, the curves of compounds **2**−**6** clearly indicate that all compounds are quite robust. Thermal degradation of purine complexes (**2**−**4**) does not show discrimination of the lost weight attributable to the coordinated water molecule and the pyrolysis of the organic molecules. They remain stable up to 250 (**2**), 270 (**3**), and 220 °C (**4**), and the coordinated water molecule is only released with the breakdown of the overall structure

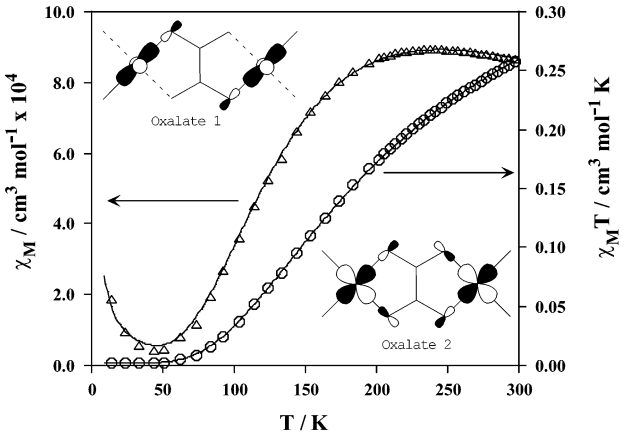

Figure 6. Temperature dependence of χ_M(△) and χ_MT (○) for compound **1**, showing the theoretical fit (−) for an antiferromagnetic dimer (see text).

which takes place through successive decomposition processes leading to the formation as final residues of Co_3O_4 above 410 °C for cobalt(II) complexes and ZnO above 550 °C for **3**.

The metal-organic framework of adenine complexes **5** and **6** retains its rigidity and stability up to 190 °C. The first weight loss is attributable to the loss of the crystallization water molecule (exp. 3.4%, calc. 3.1% for **5**; exp. 3.3%, calc. 3.1% for **6**). The dehydration temperature falls with the higher range of values reported for the release of the crystallization water molecules probably owing to the robustness of the hydrogen-bonding environment around the O6w atom in the above-described crystal structure of these complexes. The large crystals do not change their external morphology during their dehydration, but X-ray diffraction profiles from single crystals and polycrystalline samples show a significant peak broadening and loss of intensity during dehydration. This fact indicates a significant loss of crystallinity during the first thermal degradation process and the crucial role of free water molecules in supporting the overall supramolecular three-dimensional architecture. The loss of the coordinated water molecule takes place above 250 °C. The resulting compounds are unstable, and they undergo a progressive mass loss to lead Co_3O_4 and ZnO at 390 and 540 °C, respectively. These thermoanalytical data indicate the quite robust cohesiveness of the crystal structures.

Magnetic Properties. The χ_MT and χ_M vs T curves (χ_M is the magnetic susceptibility per copper atom) for compound **1** are shown in Figure 6. The χ_MT value is 0.258 cm^3 mol^{-1} K at room temperature, decreasing markedly upon cooling up to a value of 0.002 cm^3 mol^{-1} K at 50 K. Below this temperature, this value remains practically constant owing to the presence of a small amount of paramagnetic impurities. The χ_M curve shows a maximum at 230 K, indicating that significant overall antiferromagnetic coupling is involved.

Previous experimental and theoretical studies have demonstrated the remarkable capability of the bis-bidentate oxalato ligand to mediate electronic effects between paramagnetic metal ions.[42] For oxalato-bridged Cu(II) complexes it has been found that the value and type of the magnetic coupling is essentially governed by the magnitude of the

(39) Salam, M. A.; Aoki, K. *Inorg. Chim. Acta* **2001**, *314*, 71.
(40) (a) Amantia, D.; Price, C.; Shipman, M. A.; Elsegood, M. R. J.; Clegg, W.; Houlton, A. *Inorg. Chem.* **2003**, *42*, 3047. (b) Gibson, A. E.; Price, C.; Clegg, W.; Houlton, A. *J. Chem. Soc., Dalton Trans.* **2002**, 131.
(41) (a) Jalbout, A. F.; Adamowicz, L. *J. Phys. Chem. A.* **2001**, *105*, 1033. (b) Sukhanov, O. S.; Shishkin, O. V.; Gorb, L.; Podolyan, Y.; Leszczynski, J. *J. Phys. Chem. B* **2003**, *107*, 2846.

overlap between the symmetry adapted highest occupied molecular orbitals (HOMOs, σ symmetry) of the oxalato ligand and the metal-centered magnetic orbitals (mainly, a $d_{x^2-y^2}$ type in square-planar, square-pyramidal, and tetragonally elongated octahedral geometry) which are defined by the short equatorial (or basal) copper-ligand bonds. The strongest antiferromagnetic couplings (values of J ranging from -260 to -400 cm^{-1})[43] result when the oxalato bridge is symmetrically coordinated with two short bond distances at each copper(II) and, so that, it is coplanar with the magnetic orbitals. But when one copper-bridge distance is long, the two metal-centered magnetic orbitals are parallel to each other and perpendicular to the bridging ligand and the magnetic coupling through oxalato is substantially reduced (J ranging from $+10$ to -50 cm^{-1}).[7−9,44] Both orbital topologies alternate regularly along the polymeric chain of **1**. The centrosymmetric *ox2* bridge (containing the O3, O4, C10 atoms) is attached to the copper centers with two short Cu−O bond distances (<2.02 Å), leading to an almost planar Cu-*ox2*−Cu framework. The *ox1* ligand (containing the O1, O2, C9 atoms) is asymmetrically coordinated with a bond distance (Cu−O1: 2.277(2) Å) significantly longer than the other one (Cu−O2: 1.967(2) Å), and the dihedral angle between the oxalato and the mean equatorial plane of the CuO_4O_wN chromophore is 86.8°. Taking into account these structural features, the magnetic data of compound **1** were fitted to an antiferromagnetic Heissenberg S = 1/2 alternating chain model[45] derived through the Hamiltonian $H = -J\Sigma[S_{2i}S_{2i-1} + \alpha S_{2i}S_{2i+1}]$ [α is the alternating parameter and $S_{2i-1} = S_{2i} = S_{2i+1} = 1/2$]. The best-fit parameters obtained by least-squares fit are $J = -268.8$ cm^{-1}, $\alpha J = -0.6$ cm^{-1}, $g = 2.14$ with the agreement factor $R = 6.8 \times 10^{-5}$ (R is defined as $R = \Sigma_i((\chi_M)_{obs}(i)-(\chi_M)_{calc}(i))^2/\Sigma_i((\chi_M)_{obs}(i))^2$. The calculation was limited to the data points above 100 K, since below $kT/|J| = 0.25$ the theoretical results of the alternating chain model are unreliable. Given this fact and the small value of the α parameter, the magnetic data of compound **1** have also been fitted by the Bleaney−Bowers expression[46] for the magnetic susceptibility of isotropically coupled dinuclear S = 1/2 ions, based on spin Hamiltonian $H = -JS_AS_B$, adding an impurity term (ρ) defined as the molar fraction of noncoupled species. It is assumed that the paramagnetic impurity obeys the Curie Law and has the same molecular weight and the same g factor as those of the main compound. The results of the fit were as follows: $J = -274.4$ cm^{-1}, $g = 2.16$, $\rho = 0.05$, and $R = 5.7 \times 10^{-4}$. The antiferromagnetic interaction is similar to that (-274 cm^{-1}) reported for the dimer $[Cu_2(\mu\text{-oxalato})(L)_2](Ph_4B)_2$ (L = N,N′,N″-triallyl-1,4,7-triazaciclononane),[47] and it falls in the lower limit of the range found for oxalato-bridged complexes characterized by a planar Cu-ox-Cu core. Other features such as the basicity of the terminal ligands and structural distortions (especially those involving deviations from the planarity of the metal ion with respect to the mean plane of the bridging ligand of the basal plane) can play a key role in the fine-tunning of the exchange coupling.

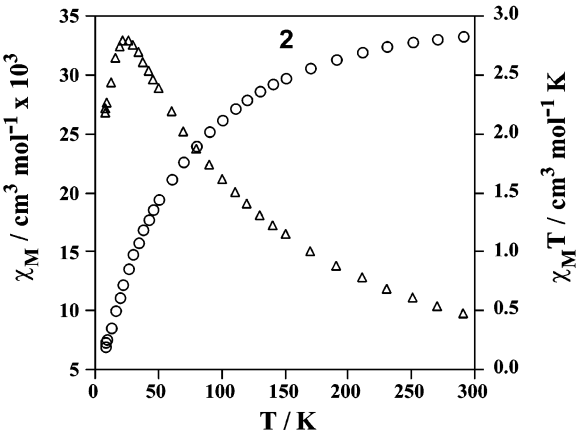

Figure 7. Temperature dependence of χ_M(△) and χ_MT (○) for compound **2**.

The magnetic properties of cobalt(II) complexes (**2**, **4**, and **5**) were measured at a magnetic field of 1000G, and they show a similar behavior (see Supporting Information). A plot of the thermal dependence of the molar magnetic susceptibility for compound **2** is represented in Figure 7. The χ_M curve increases when the compound is cooled until a maximum is reached at 24 K with a value of 0.033 cm^3 mol^{-1} and then decreases very quickly. The $\chi_M T$ curve exhibits a continuous decrease upon cooling. This behavior is indicative of a moderate antiferromagnetic coupling between the cobalt(II) centers through the bridging oxalato ligand. The room-temperature moment of 4.77 μ_B is on the range observed for high-spin octahedral cobalt(II) complexes[7,8,48] and is much larger than the spin-only value of 3.86 μ_B (with $g = 2.0$) for an uncoupled high-spin cobalt(II) ion (with S = 3/2) indicating that an important orbital contribution is involved.

The quantitative analysis of magnetic properties for systems involving ions with a significant orbital contribution is a difficult task. All our attemps to reproduce the

(42) (a) Kahn, O. *Comments Inorg. Chem.* **1984**, *3*, 105. (b) Alvarez, S.; Julve, M.; Verdaguer, M. *Inorg. Chem.* **1990**, *29*, 4500. (c) Cano, J.; Alemany, P.; Alvarez, S.; Verdaguer, M.; Ruiz, E. *Chem. Eur. J.* **1998**, *4*, 476. (d) Cabrero, J.; Ben Amor, N.; de Graaf, C.; Illas, F.; Caballol, R. *J. Phys. Chem. A* **2000**, *104*, 9983.

(43) (a) Julve, M.; Verdaguer, M.; Kahn, O.; Gleizes, A.; Philoche-Levisalles, O. *Inorg. Chem.* **1983**, *22*, 368. (b) Julve, M.; Verdaguer, M.; Kahn, O.; Gleizes, A.; Philoche-Levisalles, O. *Inorg. Chem.* **1984**, *23*, 3808. (c) Julve, M.; Faus, J.; Verdaguer, M.; Gleizes, A. *J. Am. Chem. Soc.* **1984**, *106*, 8306. (d) Bencini, A.; Fabretti, C.; Zanchini, C.; Zannini, P. *Inorg. Chem.* **1987**, *26*, 1445. (e) Castillo, O.; Muga, I.; Luque, A.; Gutiérrez-Zorrilla, J. M.; Sertucha, J.; Vitoria, P.; Román, P. *Polyhedron* **1999**, *18*, 1237.

(44) (a) Fitzgerald, W.; Foley, J.; McSweeney, D.; Ray, N.; Sheahan, D.; Tyagi, S. *J. Chem. Soc., Dalton Trans.* **1982**, 1117. (b) Oshio, H.; Nagashima, U. *Inorg. Chem.* **1992,** *31*, 3295. (c) Suárez-Varela, J.; Domínguez-Vera, J. M.; Colacio, E.; Avila-Rosón, J. C.; Hidalgo, M. A.; Martín-Ramos, D. *J. Chem. Soc., Dalton Trans.* **1995**, 2143. (d) Smekal, Z.; Travnicek, Z.; Lloret, F.; Marek, J. *Polyhedron* **1999**, *18*, 2787. (e) Calatayud, M. L.; Castro, I.; Sletten, J.; Lloret, F.; Julve, M. *Inorg. Chim. Acta* **2000**, *300*, 846.

(45) (a) Duffy, W.; Bart, K. P. *Phys. Rev.* **1968**, *165*, 647. (b) Hall, J. W.; Marsch, W. E.; Weller, R. R.; Hatfield, W. E. *Inorg. Chem.* **1981**, *20*, 1033.

(46) Bleaney, B.; Bowers, K. D. *Proc. R. Soc. London Ser. A* **1952**, *214*, 451.

(47) Farrugia, L. J.; Lopinski, S.; Lovatt, P. A.; Peacock, R. D. *Inorg. Chem.* **2001**, *40*, 558.

(48) (a) Zhang, W.; Jeitler, J. R.; Turnbull, M. M.; Landee, C. P.; Wei, M.; Willet, R. D. *Inorg. Chim. Acta* **1997**, *256*, 183. (b) De Munno, G.; Poerio, T.; Julve, M.; Lloret, F.; Viau, G. *New J. Chem.* **1998**, 299.

experimental susceptibility data of the cobalt(II) complexes by using the classical spin Heissenberg chain model[49] with $S = 3/2$ or by fitting the low-temperature data as collections of Ising chain $S = 1/2$ effective spins with antiferromagnetic interactions[50] were unsuccessful. However, it is interesting to notice that the magnetism curves for the complexes **2**, **4**, and **5** are similar to those found for polynuclear oxalato bridged cobalt(II) complexes with J values up to -25 cm^{-1}.[51] There are no known examples where the oxalate mediates a ferromagnetic interaction.

Acknowledgment. This work was supported by the Spanish Ministerio de Ciencia y Tecnología (MAT2002-03166) and the Universidad del Pais Vasco/Euskal Herriko Unibertsitatea (9/UPV 00169.310-15329/2003). J.P.G. and U.G. thank these institutions for predoctoral fellowships.

Supporting Information Available: X-ray crystallographic files in CIF format and tables of hydrogen bonds and aromatic interactions, magnetic data, and thermal curves. This material is available free of charge via the Internet at http://pubs.acs.org.

IC049569H

(49) (a) Fisher, M. E. *J. Math. Phys.* **1963**, *4*, 124. (a) Fisher, M. E. *Am. J. Phys.* **1964**, *32*, 343.

(50) (a) Abragam, A.; Bleaney, B. *Electron Paramagnetic Resonance of Transition Ions*; Dover: New York, 1970. (b) Kahn, O. *Molecular Magnetism*; VCH: New York, 1993.

(51) (a) Van Kralingen, C. G.; Van Ooijen, J. A. C.; Reedjijk, J. *Trans. Met. Chem.* **1978**, 90. (b) Glerup, J.; Goodson, P. A.; Hodgson, D. J.; Michelsen, K. *Inorg. Chem.* **1995**, *34*, 6255. (c) Hursthouse, M. B.; Light, M. E.; Price, D. J. *Angew. Chem., Int. Ed.* **2004**, *43*, 472.